# A Distribution Law for Free-Tropospheric Relative Humidity

STEVEN C. SHERWOOD

*Yale University, New Haven, Connecticut*

E. ROBERT KURSINSKI

*The University of Arizona, Tucson, Arizona*

WILLIAM G. READ

*Jet Propulsion Laboratory, California Institute of Technology, Pasadena, California*

## ABSTRACT

The probability distribution of local relative humidity $\mathcal{R}$ in the free troposphere is explored by comparing a simple theoretical calculation with observations from the global positioning system (GPS) and the Microwave Limb Sounder (MLS). The calculation is based on a parcel of air that conserves its composition during diabatic subsidence, until it is resaturated by randomly entering a convective system. This simple "advection–condensation" model of relative humidity predicts a probability density for $\mathcal{R}$ proportional to $\mathcal{R}^{r-1}$, where $r$ is the ratio of time scales associated with subsidence drying and random moistening. The observations obey this distribution remarkably well from 600 to 200 hPa in the Tropics and midlatitudes; possible reasons for this are discussed. The lowest values of $\mathcal{R}$ are predicted, and observed, to be the most probable. The observed vertical variation of $\mathcal{R}$ is well explained by that of the subsidence time scale, which is set by large-scale dynamics and radiation. These results imply that cloud microphysics exerts little control on water vapor's greenhouse effect, but that relatively subtle dynamical changes have the potential to alter the strength of its feedback on climate change.

## 1. Introduction

Water vapor is presently the earth's strongest greenhouse gas, but unlike others is controlled internally by the climate system on a short time scale (see Held and Soden 2000). Thus, one of the most pressing problems in predicting climate sensitivity is understanding how this control operates. As temperature rises, multiphase constituents such as water increasingly prefer the vapor phase, with equilibrium ("saturated") vapor pressure rising between 6% $(°C)^{-1}$ and 18% $(°C)^{-1}$ at present terrestrial temperatures. When using models lacking an explicit hydrologic cycle, most previous investigators of climate sensitivity (beginning with Arrhenius 1896) assumed that actual concentrations would change at this same rate in a climate change, in effect assuming that

relative humidity would remain invariant. This expectation is now supported by numerical climate models (GCMs) in which humidity is calculated rather than assumed (Held and Soden 2000; Soden and Held 2006), and by some compelling observational studies (Soden et al. 2002, 2005). The resulting feedback approximately doubles the sensitivity of climate to any exogenous forcing.

A major sticking point is that condensed water is usually absent, and water vapor pressure consequently below equilibrium almost everywhere in the atmosphere.[1] Departures from equilibrium are most pronounced in the subtropical "free troposphere" where relative humidity is often well below 10%. Such radical

---

*Corresponding author address:* S. Sherwood, Yale University, New Haven, CT 06520.
E-mail: ssherwood@alum.mit.edu

---

[1] It is now becoming evident that water vapor mixing ratios at temperatures below about −50°C are frequently above saturation. The reasons for this are not understood at this time, but the occurrence of supersaturation only adds to the concern about assuming that relative humidity is climate invariant.

departures demand a theory of relative humidity since even a modest climate sensitivity of relative humidity could significantly change the strength of the feedback (Pierrehumbert 1995; Spencer and Braswell 1997). This is because (as with carbon dioxide) absorption depends roughly on the logarithm of the concentration: halving the relative humidity from 10% to 5% has about the same impact as going from 100% to 50%.

Outgoing clear-sky radiation in GCM climate-change simulations is broadly consistent with relative humidity preservation, but neither these nor the observational studies have put the issue to rest. Water vapor concentrations are controlled both by advection on all scales and by moistening by falling hydrometeors, making water vapor a challenging problem. It is possible that GCMs are too diffusive or that their crudely represented cloud microphysics will not respond realistically to climate change. Of greatest concern is the free troposphere of the Tropics and subtropics where the water vapor feedback is strongest, cloud physics may have greatest leverage, and departures from equilibrium are greatest (Held and Soden 2000). The observational studies show that the feedback is nontrivial, but could be consistent with a broad range of feedback strengths. Until a testable, straightforward, heuristic explanation can be given as to why large departures from equilibrium occur and why these should be climate invariant, complex model results alone will remain unconvincing.

A useful paradigm has emerged in the past decade to explain observed water vapor distributions in the free troposphere, known as the time-of-last-saturation or the *advection–condensation* model (Pierrehumbert et al. 2006). The basic idea is that water vapor is set to its saturation value (or some value close to this) when an ascending air parcel cools sufficiently to exceed saturation, and the mixing ratio subsequently remains unchanged if the parcel temperature stays the same or increases, until it comes in contact with the mixed layer or is entrained into another cloud system. Thus, a parcel's humidity will equal the lowest saturation value it has experienced since leaving the boundary layer. This was first tested by Sherwood (1996) against radiosonde and Special Sensor Microwave Temperature-2 (SSMT/ 2) humidity fields in the tropical free troposphere in an Eulerian calculation with observed winds where a relative humidity ceiling slightly below saturation was assumed for mesoscale regions $O[(100 \text{ m})^2]$. Further tests of the idea with Lagrangian calculations confirmed that a 100% saturation could be assumed with accurate results all the way to 150 hPa (Dessler and Sherwood 2000; Pierrehumbert and Roca 1998; Salathé and Hartmann 1997); such calculations have proven useful for diagnosing water vapor distributions in better detail

than they can be observed (Roca et al. 2005). Folkins et al. (2002) also showed that, even without explicit wind information, the tropical mean vertical profile of relative humidity from 11 to 14 km could be obtained simply by enforcing energy and mass conservation.

In none of these calculations did moistening by re-evaporating hydrometeors play any role, except implicitly by helping to establish the saturation constraint applied to the coldest parts of a parcel's trajectory. Even the observed tendency of cloudy air to maintain higher moisture content than clear air (Soden 1998) can be explained on the basis of the cloud's radiative impact on air trajectories without invoking cloud water sublimation, which is of secondary importance (Sherwood 1999). These results are plausible since >99% of atmospheric water is in the vapor phase. Condensed water mixing ratios are significant compared to vapor mixing ratios only where thick cloud cover is present, a small fraction of the free troposphere. In tropical air columns with optically thick cold clouds, average relative humidity at all levels is typically 80%–90% (Sherwood 1996), in reasonable accord with the model. While clouds persist for some time outside of convective systems, most of the water condenses out in much less than one day, which is short compared to the ~10 day lifetime of water vapor. Thus, evaporation of these hydrometeors helps to bring the small, "convective" part of the atmosphere near saturation but evidently has minor impact elsewhere.

Both Lagrangian and Eulerian tests of this model do suffer from three limitations. First, the wind field is only known at coarse resolution, so individual trajectories will not execute the detailed mesoscale motions occurring in nature. Second, vertical velocities are unobserved, must be inferred indirectly, and are inaccurate, yet are the most powerful influence on a parcel's relative humidity. Third, the humidity observations required to test the calculations have their own inaccuracies. In the case of radiosondes these include biases that can exceed a factor of 2 for some models (Soden et al. 2004) as well as random errors. For nadir-view satellite retrievals the main problems are very coarse vertical resolution, moisture-dependent vertical sampling, and inability to retrieve accurately in cloudy conditions (e.g., Lanzante and Gahrs 2000). Recent instrumentation has improved this situation somewhat, achieving point accuracies of 10%–25% (Gettelman et al. 2004; Wu et al. 2005) in clear and partly cloudy conditions. Limb sounders suffer from sparse sampling and less-than-ideal horizontal resolution. No single platform is able to "image" the full relative humidity field accurately in four dimensions.

A more fundamental limitation of the advection–

condensation paradigm is that it is incomplete without a sufficient description of the wind field. An explicit four-dimensional description is cumbersome, inelegant, and lacks predictive utility. Yet certain statistics of a tracer field are often informative without having to know the advection field explicitly. For example, Tuck et al. (2003) assessed the importance of different near-tropopause mixing processes from two-point humidity correlation statistics. Previous investigators have found exponential distributions of humidity near the tropopause (Gierens et al. 1999; Spichtinger et al. 2002). Soden and Bretherton (1993) noted an approximately lognormal distribution of upper-tropospheric humidity (an average from about 200 to 500 hPa, though with a humidity-dependent weighting function). As yet no unequivocal explanation for these distributions has emerged. Complicating the picture, Zhang et al. (2003) reported bimodal distributions in some (but not all) available datasets. Previous studies agree, however, that water vapor mixing ratio and relative humidity distributions are very broad and look nothing like the Gaussian distribution often found for other geophysical quantities. This indicates that water vapor equilibria are not maintained by random additions and subtractions of water from air parcels, which should (by instituting a random walk of humidity) produce a Gaussian distribution.

We begin this study by formulating the advection–condensation model more explicitly, idealizing the motions of a candidate parcel of air. This predicts a relative humidity distribution, which we then compare to observations.

## 2. A steady-state, diabatic advection–condensation model

### a. Diabatic motion and parcel relative humidity

The dominant circulation in the Tropics is a "wet up, dry down" overturning. Dynamic adjustment is rapid near the equator, isentropic temperature gradients are modest, and synoptic upper-air variations are typically no more than a few degrees. Thus, we may idealize the life of a free-tropospheric parcel of air in the Tropics by saying that it rises in a convective updraft, detrains at some level (possibly, but not necessarily near the tropopause), then meanders through the troposphere quasi horizontally until either reaching the boundary layer or being entrained into some other convective system. Complications of this simple picture will be discussed in section 4.

During this meandering, the parcel experiences a net radiative cooling, causing it to sink gradually through isentropic surfaces. Since these surfaces fluctuate little

in temperature, the result is a strong tendency toward a gradual compressive increase of the parcel's temperature (albeit with some fluctuations superimposed on this). The Clausius–Clapeyron equation dictates that the parcel's saturation mixing ratio $q_s$ grow according to

$$\frac{Dq_s}{Dt} = q_s\left(\frac{-L_v w \Gamma}{R_v T^2}\right), \tag{1}$$

where $Dq_s/Dt$ is the material derivative following the sinking parcel, $T$ is the local temperature, $w$ the (negative) vertical velocity, $\Gamma$ the (positive) lapse rate, and $R_v$ and $L_v$ the water vapor gas constant and latent heat of vaporization. Since clear-sky radiative cooling rates in the tropical atmosphere are nearly height invariant from the boundary layer to about 250 hPa (e.g., Folkins et al. 2002) and other quantities also retain similar magnitudes, it is not a drastic approximation to treat the quantities in parentheses as constant and then integrate, yielding an exponentially growing $q_s$:

$$q_s(t) \approx q_s(0) \exp\left(-\frac{L_v w \Gamma}{R_v T^2} t\right). \tag{2}$$

A key assumption of the advection–condensation model is that, during this process, the water vapor mixing ratio $q$ itself is conserved. This means that the relative humidity $\mathcal{R} = q/q_s$ must decrease exponentially in time. By setting $t = 0$ when the parcel was last saturated, we obtain

$$\mathcal{R} \approx \exp\left(-\frac{t}{\tau_{\text{Dry}}}\right), \tag{3}$$

where we define the subsidence *drying time* constant

$$\tau_{\text{Dry}} \equiv \frac{R_v T^2}{L_v w \Gamma} \tag{4}$$

(note that "drying" here refers only to relative humidity, not to absolute humidity, which remains constant). We may interpret $t$ as the "age" of the air parcel; $\mathcal{R}$ directly measures this age in a manner analogous to how the ratio of $^{14}C$ to $^{12}C$ measures the age of an organic carbon sample. Visual inspection of geostationary water vapor imagery loops (which indicates upper-tropospheric $\mathcal{R}$ rather than $q$) confirms that pockets of air become successively drier as they meander along, until they encounter fresh convective activity. The subsidence drying time $\tau_{\text{Dry}}$ is of the order of days, varying with height (Mapes 2001).

### b. Remoistening and a distribution law for relative humidity

The distribution of $\mathcal{R}$ must clearly depend on that of parcel "age" $t$. Now suppose that parcels are "remoist-

ened" by encounters that occur randomly with a fixed probability per unit time independent of previous history (a Poisson process). The probability distribution of intervals between events in a Poisson process is exponential. Therefore, the distribution of ages $t$ among air parcels outside convection at any given moment will be

$$P_t(t) = \frac{1}{\tau_{\text{Moist}}} \exp\left(-\frac{t}{\tau_{\text{Moist}}}\right). \tag{5}$$

The decay constant $\tau_{\text{Moist}}$ is the reciprocal of the remoistening probability per unit time.

If we assume that the troposphere is very deep with constant $w$, $\tau_{\text{Dry}}$, and $\tau_{\text{Moist}}$ at all heights at and above the level under investigation, the model becomes stationary and ergodic, with the same calculation applying equally well to the distribution of $t$ on parcels initialized (remoistened) at a given time and level, or parcels observed at a given time and level. Clearly this assumption will fail near the tropopause where there is a limit to how old/dry the air can be. But, since the free troposphere is roughly seven times as thick as a typical water-vapor scale height, the "unbounded" approximation should be acceptable except very close to the tropopause.

Combining (5) with (3) we obtain the distribution of relative humidity away from hydrometeors,

$$P_{\mathcal{R}}(\mathcal{R}) \propto \mathcal{R}^{r-1},$$

$$r = \frac{\tau_{\text{Dry}}}{\tau_{\text{Moist}}}. \tag{6}$$

This one-parameter family of curves describing the distribution of $\mathcal{R}$ is a momentous result. The two time scales appear only as a ratio. If $r = 1 (\tau_{\text{Dry}} = \tau_{\text{Moist}})$, we obtain a uniform distribution between 0 and 1. Otherwise, we get a broad distribution peaking either at $\mathcal{R} = 0$ (for $\tau_{\text{Dry}} < \tau_{\text{Moist}}$) or 1 (for $\tau_{\text{Dry}} > \tau_{\text{Moist}}$). Distributions are predicted to be broad regardless of $r$. We may integrate (6) to yield an even simpler, cumulative distribution

$$C(\mathcal{R}) = \mathcal{R}^r. \tag{7}$$

We prefer the cumulative distribution to the density because the former is a unique function while the latter depends on the humidity measure used (see Pierrehumbert et al. 2006).

## 3. Observations

To test (7), we ideally need a tropical (or global) moisture dataset with (i) unbiased, preferably complete, geographic sampling and (ii) reliable accuracy throughout the full range of relative humidities in the atmosphere. Aircraft and radiosonde data lack the uniform spatial coverage and/or accuracy required for this job. While current-generation infrared sounder data could probably be useful, most pixels are cloud contaminated and retrievals depend on model-based initial guesses, both of which may introduce biases. We have not explored such datasets here. Instead, we employ satellite limb observations to obtain the necessary spatial sampling and vertical resolution. These limb observations employ sufficiently long wavelengths to penetrate most clouds. One drawback of limb observations is that they represent long ($\sim$100–300 km) horizontal path averages. This may smooth the distribution somewhat, particularly at the moist end where convective sources provide small-scale structure. However, geostationary imagery shows that the dry regions of greatest concern are typically characterized by scales larger than this (notwithstanding the occasional moist filament that may appear).

### a. Global positioning system (GPS)

GPS occultations can be used to obtain path integrals of atmospheric refractivity $N$, which is determined primarily by the density (concentration) of air and its water vapor concentration (e.g., Kuo et al. 2004; Kursinski et al. 1997; Steiner and Kirchengast 2005). The refractivity $N$ is little affected by clouds. Because water vapor concentrations decrease rapidly with temperature, $N$ is essentially unaffected by water vapor below $\sim$230 K. At temperatures above $\sim$240 K water vapor concentration can be retrieved, as long as the dry-air density contribution to $N$ is known from independent data. With information on pressure and temperature, this can be converted to relative humidity $\mathcal{R}$. Here, we present retrievals from the German Challenging Minisatellite Payload (CHAMP) satellite from October 2001 and January, April, and July 2002 [for a comparison of results from the satellites CHAMP and SAC-C, see Hajj et al. (2004)]. Moisture is calculated at the University of Arizona based on refractivities from the Jet Propulsion Laboratory (JPL) occultation retrieval system. The occultation sampling is globally distributed with 2000–3000 profiles per month. Independent information on the temperature profile, and a stratospheric geopotential boundary condition for hydrostatic integration, is derived from European Centre for Medium-Range Weather Forecasts (ECMWF) operational analyses. Any biases in these data, particularly temperature, will affect those of $\mathcal{R}$. We calculate $\mathcal{R}$ with respect to the liquid or ice phase at temperatures above or below freezing, respectively.

Our retrievals follow the procedure outlined by

Kursinski and Hajj (2001), with two modifications. The primary modification is a correction for diffraction according to Gorbunov (2002). This correction improves accuracy, reduces multipathing problems, and permits vertical resolution of approximately 200 m. Horizontal resolution in the along-track direction is about 300 km. We estimate the accuracy of individual retrievals at low tropical altitudes to vary from 2% at low $\mathcal{R}$ to 10% at high $\mathcal{R}$. This increases to ~15% at the highest altitudes where retrievals were attempted. These uncertainties include error in the input temperature and pressure information as well as the retrieved refractivity. A more thorough description of the methodology and evaluation of CHAMP and SAC-C water vapor retrievals is in preparation.

This method does not ensure that individual retrievals will be positive. To avoid negative values in the histograms, we have for the time being adopted the simple approach of pushing any negative RH values up to the lowest positive histogram bin (0%–2.5%). This unfortunately causes some distortion to values at the very dry end of the spectrum, but its effect on most of the histogram will be insignificant. A deconvolution method for estimating the true distribution of $\mathcal{R}$ values, given the observed distribution and independent noise estimates, is still under development.

To generate the relative humidity histograms [probability density functions (PDFs)], we first separated the data into latitude versus height intervals, 0.5 km thick and 10° in latitude, spanning from 2- to 9-km altitude and 30°S–30°N latitude. The relative humidity bins are 10% wide (e.g., 80%–90%) except in the 0%–10% relative humidity interval, which is divided into four equally spaced bins, each 2.5% wide. The finer bin spacing at low relative humidities is because very low relative humidity values occur rather frequently, and smaller absolute differences become more important radiatively. The second modification to the method of Kursinski and Hajj (2001) is that, instead of making a yes-or-no retrieval decision for each individual occultation (based on temperature), a decision was made for each altitude bin and was adhered to for all retrievals in that bin. This ensures that histograms are not distorted by data selection biases.

### b. Microwave Limb Sounder (MLS)

The original MLS instrument flew on board the *Upper Atmosphere Research Satellite* (*UARS*), observing microwave limb emission useful for detecting a variety of trace species. Though this instrument was not specifically designed to measure water vapor except in the stratosphere, an upper-tropospheric retrieval (V4.9)
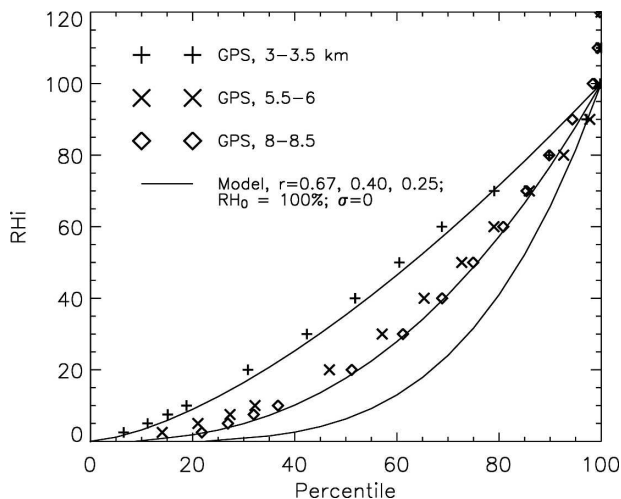


FIG. 1. Cumulative distributions of $\mathcal{R}$ at three levels in the lower and middle troposphere from GPS data (symbols) and from the stochastic parcel model with three values of $r$ (lines), where $r$ decreases as the curves shift to the lower right.

was developed (Read et al. 2001) based on modeled radiances and National Centers for Environmental Prediction (NCEP) reanalysis temperatures. This retrieval performed reasonably well in comparison with other instruments, though it showed dry biases below 147 hPa. We show here the distribution of all available V4.9 data from 1993 for retrieval levels 464, 316, and 215 hPa.

The successor to this instrument, Earth Observing System (EOS) MLS, is carried on the *Aura* satellite launched in late 2004 (Waters et al. 2006). This newer instrument was equipped with additional spectrometers to enable a better upper-tropospheric retrieval, using contrast between multiple wavelengths, and appears to be performing well (Froidevaux et al. 2006). Another difference is that temperature is retrieved simultaneously by the instrument. Since both versions of the MLS water vapor retrieval are logarithmic, negative values cannot occur. EOS retrievals are not attempted at 464 hPa owing to attenuation of the signal, at least in the current version (1.51), but should be more accurate at the remaining levels of the *UARS* product. We show EOS MLS retrieval distributions from 1 August 2004 to 7 July 2005. The impact of retrieved temperature in the EOS MLS was checked by recomputing results using NCEP temperatures; the difference was found to be small compared to *UARS*–EOS differences.

### c. Observed histograms

Figure 1 shows the cumulative distributions of relative humidity from GPS at three levels. The distributions indicate not only a broad spread of observed hu-
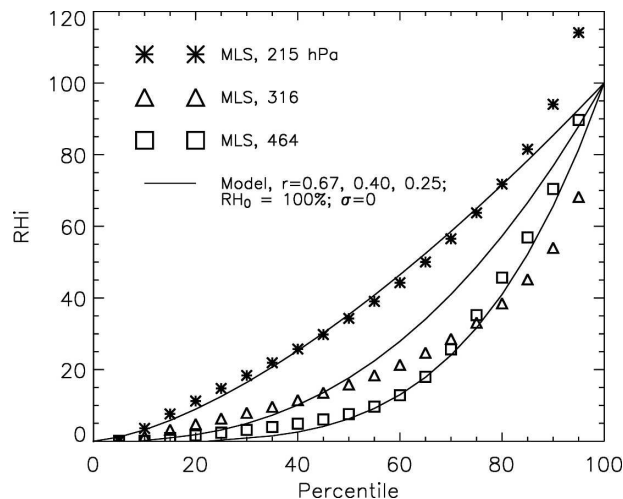
FIG. 2. As in Fig. 1, except using data from the *UARS* MLS for the upper troposphere.



FIG. 3. As in Fig. 2, except using data from the EOS MLS.

midity values, but also a large fraction of observations of very dry air. One-quarter of the tropical air at 8 km is below 4% relative humidity. Relative humidity decreases with altitude over the available range.

These observed distributions are compared with predictions of the stochastic parcel model for several candidate values of $r$. The distributions are quite close to the predicted curves. There is some tendency of flattening toward the moist end, especially at 3 km, indicating that the moistest values are not quite as moist as predicted. This may well be due to the averaging along paths, which will intersect mixtures of cloudy and clear sky even in the cloudiest conditions. The agreement at 3 km is still surprisingly good, given that one might expect the assumptions of the model to be violated by shallow cumulus moistening.

Figures 2 and 3 show similar tropical results from *UARS* and EOS MLS, respectively. At 215 hPa, data from the older *UARS* instrument agree well with the stochastic model, but this is less true for the EOS data where dry values are not as dry as with *UARS*. This level is sufficiently close to the tropopause that the lowest plausible water vapor mixing ratio (that typical of the cold point) corresponds to $\mathcal{R} \approx 2\%-3\%$, which is more consistent with the newer data. Thus, the *UARS* agreement at the low end is fortuitous: the 215-hPa level is too close to the tropopause for the dry tail to extend as far as predicted by the unbounded model.

Closer to the midtroposphere the model should be, and apparently is, more successful. The dry bias present in the *UARS* data at 316 hPa has clearly decreased in the newer data, which conforms more closely to the model. At 464 the *UARS* MLS deviates from the model, but in a way opposite in character to that at 316
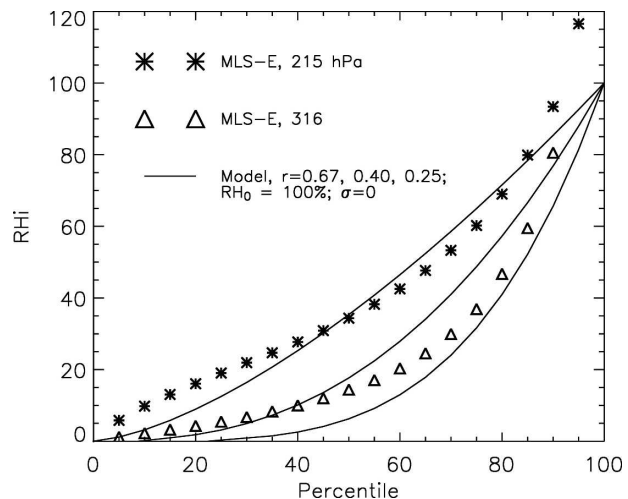
hPa, with one skewing to high $\mathcal{R}$ and the other skewing to low $\mathcal{R}$. This suggests that retrieval errors (which are often anticorrelated at nearby levels owing to overlapping weighting functions) rather than untreated physics (which would be expected to have qualitatively similar impact at these two levels) may be responsible.

Figures 4 and 5 show similar results from midlatitude data. Because of decreasing temperatures and water vapor mixing ratios, data are available from lower altitudes than in the Tropics, which limits the applicability of GPS, but also means that MLS should be more reliable at the lowest levels: 215 hPa is in the stratosphere at midlatitudes and is not shown. GPS results at 3–3.5 km are essentially identical to those in the Tropics. *UARS* MLS data obey the model at least as well at
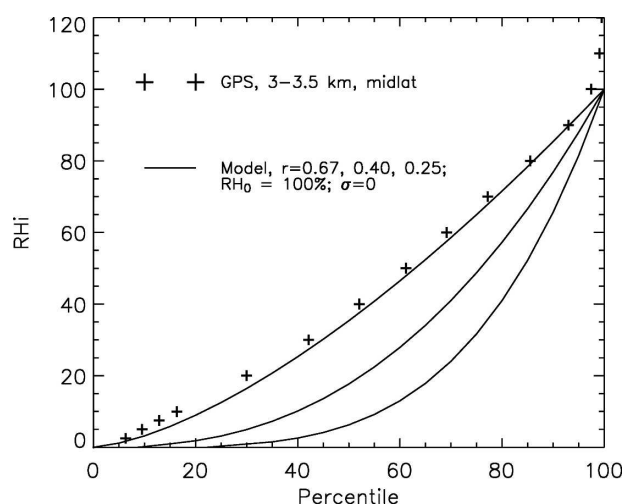


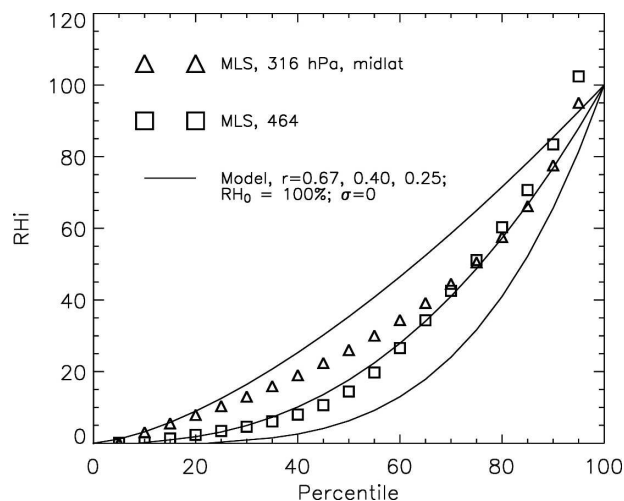FIG. 4. As in Fig. 1, except using data from 30°–60°S and 30°–60°N.

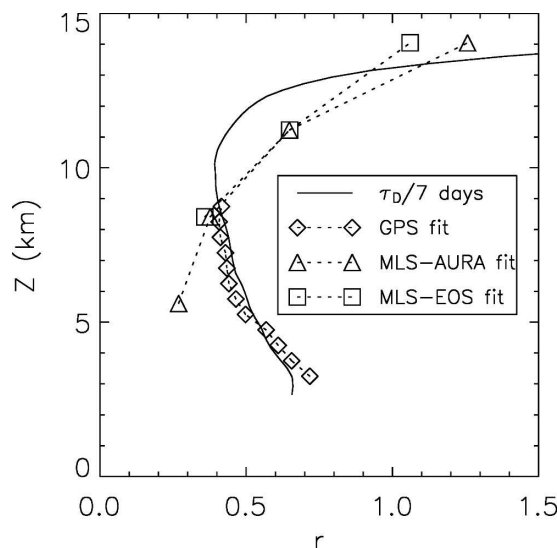FIG. 5. As in Fig. 2, except using data from 30°–60°S and 30°–60°N.



FIG. 6. Vertical variation of ratio $r$ predicted by the model and determined from the three tropical data distributions. Model-predicted $r$ is based on an assumed constant $\tau_{\text{Moist}} = 7$ days and $\tau_{\text{Dry}}$ calculated from a mean tropical observed sounding.

midlatitudes as in the Tropics, with a well-known shift toward higher $\mathcal{R}$ due mainly to isentropic transport of moist air from lower latitudes (in effect reducing $\tau_{\text{Moist}}$).

The GPS observations fail to show the atmosphere reaching saturation. While this could indicate a dry bias, it can also be plausibly explained as a result of averaging over long ($\sim$100–300 km) paths, a scale much longer than the size of a typical cloud or saturated region. It is encouraging that the maximum $\mathcal{R}$ is at least consistent at all observed levels. By contrast, the MLS observations frequently exceed ice saturation at the highest levels. Some of these high values are undoubtedly cloud artifacts, but supersaturated moisture values have been confirmed in the upper troposphere by in situ observations (e.g., Jensen et al. 2005).

### d. Comparison with previous results

The preponderance of dry air found here has been reported previously in the upper troposphere from microwave-based limb and nadir retrievals (Sandor et al. 1998; Spencer and Braswell 1997). It does not appear in geostationary water vapor imagery, which seldom shows values below 5% (Soden and Bretherton 1993). Deep vertical averaging probably obscures the true breadth of the $\mathcal{R}$ distribution in such imagery. We did not find the bimodality noted by Zhang et al. (2003); this is discussed in section 4.

Some previous studies (e.g., Pierrehumbert et al. 2006; Soden and Bretherton 1993) have predicted or observed something close to a lognormal distribution,

$$L_x(x) = \frac{1}{x\sqrt{\pi a}} e^{-\ln(x/x_0)^2/a}.$$

Our scaling distribution (6) approaches the limit $(1/\mathcal{R})$ when $r$ is taken to zero; the lognormal distribution approaches this same limit as its width $a$ is taken to infinity. Thus, when conditions are dry, (6) closely resembles the broadest possible lognormal distribution. In moister conditions, (6) retains its breadth while lognormal distributions necessarily become narrower. Observed conditions are insufficiently moist at most levels for these two distributions to be distinguishable. Near the tropopause, moisture is greater but data quality issues limit the distinction. In any case, (6) is simpler than a lognormal distribution in the sense that it has only one parameter rather than two. This makes fortuitous agreement with data less likely.

### e. The vertical profile

We have fitted a best value of $r$ to the data at each level by choosing the value consistent with the observed median $\mathcal{R}$ (Fig. 6). The fit is very robust for GPS data owing to the close agreement with theory, whereas the MLS best-fit $r$ have uncertainties of perhaps 20%–30% depending on how they are fitted. The data show a marked height dependence of moisture, with a dry minimum near 400 hPa or 7–8 km. Also shown on this figure is an estimate of $r$ found by calculating $\tau_{\text{Dry}}$ at each level from a mean tropical sounding with clear-sky net radiative cooling calculated with a radiative transfer model (for details, see Sherwood and Meyer 2006), divided by a $\tau_{\text{Moist}}$ assumed constant at 7 days. The cal-

culated $\tau_{\mathrm{Dry}}$ first decreases and then rapidly increases with height. The slow decrease arises primarily from the temperature dependence of the Clausius–Clapeyron equation, such that a given $dT/dt$ reduces $\mathcal{R}$ more rapidly; the rapid increase toward the tropopause reflects the slowdown in subsidence associated with loss of net radiative cooling.

This calculation recalls that of Folkins et al. (2002), except that in that study the age of parcels was determined from the detrainment profile required by mass balance without accounting for any other mixing, which limited it to the uppermost troposphere. A more detailed study accounting for both mechanisms (Sherwood and Meyer 2006) echoes the Folkins et al. conclusion that the required detrainment dominates over lateral mixing in supplying moisture to the uppermost troposphere. The results here show that the entire tropical profile is roughly consistent with a similar moistening rate/age distribution at *all* heights.

The vertical variations of the estimated and observed $r$ profiles are similar except for an upward shift of about 2 km in the estimated profile and an excessive amount of moisture predicted near the tropopause. The shift is expected because the estimated profile is based on local values of $w$ and $\Gamma$ while the observed moisture reflects conditions "upstream" at higher altitudes. This upstream influence should extend about one water vapor scale height or $\sim$2 km [a detailed calculation presented by Sherwood and Meyer (2006) confirms this]. Accounting for this brings the curves into good agreement, except for excessive moisture near the tropopause. That excess is not surprising either since temperature fluctuations, ignored in the model but caused in reality by transient waves and asymmetry in the mean temperature field, become significant close to the tropopause. In a background environment that is very moist due to the weak subsidence, these fluctuations cause cirrus cloud formation and dehydration, which prevent extreme humidity.

Despite these limitations, the similarity of the curves through most of the free troposphere indicates that the vertical variation of moisture can be explained on the basis of large-scale dynamics and radiation, as concluded by a few previous investigators. Similarly, the distribution at a given height is explained by the advection–condensation model. The only remaining variable unaccounted for is the overall moistening time scale $\tau_{\mathrm{Moist}}$.

## 4. Discussion

The simplicity evident here seems surprising in light of the real-world complexities that were overlooked.

The similarity of tropical and midlatitude results, in particular, is puzzling since extratropical dynamics would appear to be quite different from the "moist up, dry down" basis of the simple model. Also, no bimodality was found in the distributions; we find only a dry mode in $P_{\mathcal{R}}(\mathcal{R})$, peaking at $\mathcal{R} \approx 0$. Our distributions were highly robust, appearing similar in all four seasons (not shown).

Some of these findings could be artifacts of the satellite data. A 300-km pathlength is indeed long enough to eliminate structure from many convective systems. It seems unlikely, however, that this by itself could produce the right amount of dry air by accident when most of the moisture variability is at large spatial scales; such a problem should only smooth out any narrow bumps that might lurk in the real distribution. It also seems unlikely to cause convergence of tropical and midlatitude distributions, especially since midlatitude synoptic features should be captured better, but are modeled worse, than those in the Tropics. Finally, a spurious collapse of the results toward the predicted scaling relationship would seem to be ruled out by the deviations from this relationship near the tropopause where model assumptions break down. One feature more likely to be affected, however, is bimodality.

### a. Bimodality and moist extremes

Clouds should reduce the net radiative cooling and, therefore, $w$. Since "younger" air would be the cloudiest, this should reduce the apparent aging (drying) rate of the youngest air (Sherwood 1999). That, in turn, would lead to more near-saturated air than predicted with a constant $w$, possibly producing a second moist "mode" like the one found by Zhang et al. (2003) in many (primarily in situ) datasets. On the other hand, dynamically induced subsidence near convective centers could counteract this or even produce the opposite result.

Failure to observe a moist mode here could be attributed to path smoothing, as the near-saturated regions may often be too small to be isolated in a limb scan. Alternatively, the bimodality reported by Zhang et al. (2003) could have been an artifact of sampling biases; many of the field programs providing their data were specifically designed to observe across sharp gradients in atmospheric conditions, and the multiplatform moisture analysis that they examined could have taken on bimodality owing to the blending of in situ and satellite input data. No evidence of bimodality was reported by Gierens et al. (1999) in upper-tropospheric data gathered from routine commercial aircraft. Both the expected and actual details of moisture distribu-

tions near the moist end of the range therefore remain unclear, though they are being studied in cloud resolving models (Tompkins 2002).

### b. Extratropics and advection models

The basic assumption of our temperature model was that parcel temperature increases monotonically due to subsidence from the moment it leaves a near-saturated region. This idealization should fail outside the Tropics. In fact, even in the Tropics, much of the dry air was last saturated in the extratropics where potential temperature surfaces bend upward to much lower temperature (Galewsky et al. 2005), making the success doubly puzzling. Outside the Tropics, the experience of an individual parcel will surely be dominated by temperature changes associated with latitudinal excursions on isentropic surfaces and by transient fluctuations in baroclinic eddies (e.g., midlatitude cyclones), rather than by diabatic subsidence. This demands a different kind of conceptual model.

Pierrehumbert et al. (2006) have explored such a model, considering a parcel of air that executes an isentropic random walk in the meridional direction, retaining a water vapor mixing ratio equal to its lowest experienced saturation value. In one arrangement, parcels are initially saturated and then dry down through migration; this cannot be run to equilibrium (the end result would be $\mathcal{R} = 0$ for all parcels) but yields, after any finite time, a very broad lognormal distribution close to (6). A more realistic arrangement, numerically integrated to steady state, featured remoistening of the parcels at one boundary (the "Tropics"); this yielded more air near $\mathcal{R} = 0$ and 1 than did the initial-value arrangement, but in any case again produced a broad distribution.

If either of these midlatitude idealizations had included the effects of baroclinic disturbances or moist convection, which can bring parcels quasi randomly back to saturation without their having to change latitude, the results would undoubtedly have been closer to those of the diabatic model (6). But, the results were not all that different anyway, which is the likely key to why the observed tropical and midlatitude distributions both conform to (6). Regardless of whether the processes are diabatic or adiabatic, the temperature of the last saturation assumes a probability distribution that decays roughly exponentially with depression below the current temperature. The broad distribution characterized by (6) may arguably be regarded, therefore, as a general result of the advection–condensation paradigm. Specific evidence in support of the diabatic version of this, at least for the Tropics, lies in Fig. 6.

## 5. Conclusions

Satellite limb observations of relative humidity obey the remarkably simple, universal form $P_{\mathcal{R}}(\mathcal{R}) \propto \mathcal{R}^{r-1}$, predicted by considering a stochastically remoistened, subsiding air parcel. This is a simplified idealization of tropical behavior, but a nonsubsiding air parcel meandering on an inclined isentropic surface (an idealization of the extratropics with a tropical boundary) has been shown elsewhere to produce similar results. These may be regarded as two limiting cases of the advection–condensation paradigm for free-tropospheric moisture; real behavior at any latitude will be some mixture of them. Our evidence shows that this paradigm is well supported in both the Tropics and midlatitudes. Also, we find that very dry air is not limited to the subtropics but is equally prevalent in midlatitudes. The advection–condensation paradigm predicts that this dry air yet ties its moisture to temperatures elsewhere in the atmosphere, indicating that it will be governed by the Clausius–Clapeyron relation to the same degree as moisture in nearly saturated regions. The absence of a role in the model for cloud physics argues against this having any important impact on water vapor levels, other than indirectly through any effect it may have on cloud radiative forcing and winds.

The simple distribution derived here has a straightforward physical interpretation applicable in the Tropics. The relative humidity of air is a direct measure of its "age," or time since it was saturated. The power $r$ is a ratio of a drying time $\tau_{\mathrm{Dry}}$ to the mean age $\tau_{\mathrm{Moist}}$. The drying time is determined by the atmospheric sounding and radiative transfer; its variation with height leads to the observed humidity minimum near 400 hPa. The mean age is not predicted here but is empirically about a week at all altitudes. This height invariance makes sense as parcel age is controlled by horizontal transport, which occurs primarily through nearly barotropic features of the wind field that should affect all heights similarly. Near the tropopause, our simple model unsurprisingly begins to overestimate moisture because the emergent role of in situ dehydration in cirrus clouds is neglected. High moisture there results from decreasing subsidence rates, as concluded in earlier work.

The fact that a simple distribution form is found through most of the free troposphere suggests that the form will remain constant through modest climate changes. This means that the entire distribution of $\mathcal{R}$, if it shifts at all, will do so through changes in $r$, producing a smooth trend toward drier or moister values.

Since the drying rate should already be well captured by existing climate models, the main uncertainty in climatic changes in $\mathcal{R}$ comes from possible changes in the

mean parcel age $\tau_{\text{Moist}}$. Greenhouse trapping of water vapor $G$ and parcel age $t$ are each logarithmic in $\mathcal{R}$ and hence approximately linearly related; from (3), with $G$ in "log humidity" units,

$$G = G_0 - \frac{t}{\tau_{\text{Dry}}}.$$

Averaging over parcels and using the definition of $\tau_{\text{Moist}}$ yields

$$\Delta\langle G\rangle = -\frac{\Delta\tau_{\text{Moist}}}{\tau_{\text{Dry}}} = \frac{1}{r}\frac{\Delta\tau_{\text{Moist}}}{\tau_{\text{Moist}}}$$

if parcel lifetime changes. However, it follows from our definition of $G$ that

$$dG = \frac{dq}{q}$$

for a uniform rescaling of humidity $q$. A $1°C$ atmospheric warming would cause a $dq/q$ of about 10% in saturated conditions, and according to our model all humidities would increase in the same proportion if $r$ stayed constant. Putting the last two results together and noting that in most of the free troposphere $r \approx 0.4$, we find that the moistening caused by a $1°C$ warming could be radiatively negated (or doubled) by a 4% increase (or decrease) in $\tau_{\text{Moist}}$. We conclude that parcel lifetimes must be simulated precisely for water vapor's radiative effects to be well known; $\tau_{\text{Moist}}$ climate dependence would not have to be severe to significantly affect the strength of the water vapor feedback. This calls into question the reliability of water vapor feedback in GCMs with coarse grids. On the other hand, recent global simulations at decidedly noncoarse 3.5- and 7-km resolutions (Miura et al. 2005) yielded an overall feedback similar to that of coarser models, suggesting that parcel age may indeed be climate insensitive. Future work should focus on testing this proposition further.

## REFERENCES

Arrhenius, S., 1896: On the influence of carbonic acid in the air upon the temperature of the ground. *Philos. Mag.,* **41,** 237–276.

Dessler, A. E., and S. C. Sherwood, 2000: Simulations of tropical upper tropospheric humidity. *J. Geophys. Res.,* **105,** 20 155–20 163.

Folkins, I., K. K. Kelly, and E. M. Weinstock, 2002: A simple explanation for the increase in relative humidity between 11 and 14 km in the tropics. *J. Geophys. Res.,* **107,** 4736, doi:10.1029/2002JD002185.

Froidevaux, L., and Coauthors, 2006: Early validation analyses of atmospheric profiles from EOS MLS on the Aura satellite. *IEEE Trans. Geosci. Remote Sens.,* **44,** 1106–1121.

Galewsky, J., A. Sobel, and I. Held, 2005: Diagnosis of subtropical humidity dynamics using tracers of last saturation. *J. Atmos. Sci.,* **62,** 3353–3367.

Gettelman, A., and Coauthors, 2004: Validation of Aqua satellite data in the upper troposphere and lower stratosphere with in situ aircraft instruments. *Geophys. Res. Lett.,* **31,** L22107, doi:10.1029/2004GL020730.

Gierens, K., U. Schumann, M. Helten, H. Smit, and A. Marenco, 1999: A distribution law for relative humidity in the upper troposphere and lower stratosphere derived from three years of MOZAIC measurements. *Ann. Geophys.,* **17,** 1218–1226.

Gorbunov, M. E., 2002: Radioholographic analysis of radio occultation data in multipath zones. *Radio Sci.,* **37,** 1014, doi:10.1029/2000RS002.

Hajj, G. A., and Coauthors, 2004: CHAMP and SAC-C atmospheric occultation results and intercomparisons. *J. Geophys. Res.,* **109,** D06109, doi:10.1029/2003JD003909.

Held, I. M., and B. J. Soden, 2000: Water vapor feedback and global warming. *Annu. Rev. Eng. Environ.,* **25,** 441–475.

Jensen, E. J., and Coauthors, 2005: Ice supersaturations exceeding 100% at the cold tropical tropopause: Implications for cirrus formation and dehydration. *Atmos. Chem. Phys.,* **5,** 851–862.

Kuo, Y.-H., T.-K. Wee, S. Sokolovskiy, W. S. C. Rocken, D. Hunt, and A. Anthes, 2004: Errors based on comparisons of real GPS RO results with NWP forecasts and analyses. *J. Meteor. Soc. Japan,* **82,** 507–531.

Kursinski, E. R., and G. A. Hajj, 2001: A comparison of water vapor derived from GPS occultations and global weather analyses. *J. Geophys. Res.,* **106,** 1113–1138.

——, ——, J. T. Schofield, R. P. Linfield, and K. R. Hardy, 1997: Observing Earth's atmosphere with radio occultation measurements using the Global Positioning System. *J. Geophys. Res.,* **102,** 23 429–23 465.

Lanzante, J. R., and G. E. Gahrs, 2000: The "clear-sky bias" of TOVS upper-tropospheric humidity. *J. Climate,* **13,** 4034–4041.

Mapes, B. E., 2001: Water's two height scales: The moist adiabat and the radiative troposphere. *Quart. J. Roy. Meteor. Soc.,* **127,** 2353–2366.

Miura, H., H. Tomita, T. Nasuno, S. Iga, M. Satoh, and T. Matsuno, 2005: A climate sensitivity test using a global cloud resolving model under an aqua planet condition. *Geophys. Res. Lett.,* **32,** L19717, doi:10.1029/2005GL023672.

Pierrehumbert, R. T., 1995: Thermostats, radiator fins, and the local runaway greenhouse. *J. Atmos. Sci.,* **52,** 1784–1806.

——, and R. Roca, 1998: Evidence for control of Atlantic subtropical humidity by large scale advection. *Geophys. Res. Lett.,* **25,** 4537–4540.

——, H. Brogniez, and R. Roca, 2006: On the relative humidity of the atmosphere. *The Global Circulation of the Atmosphere,* T. Schneider and A. Sobel, Eds., Princeton, in press.

Read, W. G., and Coauthors, 2001: UARS Microwave Limb Sounder upper tropospheric humidity measurement: Method and validation. *J. Geophys. Res.,* **106,** 32 207–32 258.

Roca, R., J. P. Lafore, C. Piriou, and J. L. Redelsperger, 2005: Extratropical dry-air intrusions into the West African mon-

soon midtroposphere: An important factor for the convective activity over the Sahel. *J. Atmos. Sci.,* **62,** 390–407.

Salathé, E. P., and D. L. Hartmann, 1997: A trajectory analysis of tropical upper-tropospheric moisture and convection. *J. Climate,* **10,** 2533–2547.

Sandor, B. J., W. G. Read, J. W. Waters, and K. H. Rosenlof, 1998: Seasonal behavior of tropical to midlatitude upper tropospheric water vapor from UARS MLS. *J. Geophys. Res.,* **103,** 25 935–25 947.

Sherwood, S. C., 1996: Maintenance of the free-tropospheric tropical water vapor distribution, Part II: Simulation by large-scale advection. *J. Climate,* **9,** 2919–2934.

——, 1999: On moistening of the tropical troposphere by cirrus clouds. *J. Geophys. Res.,* **104,** 11 949–11 960.

——, and K. Meyer, 2006: The general circulation and robust relative humidity. *J. Climate,* **19,** 6278–6290.

Soden, B. J., 1998: Tracking upper tropospheric water vapor radiances: A satellite perspective. *J. Geophys. Res.,* **103** (D14), 17 069–17 080.

——, and F. P. Bretherton, 1993: Upper-tropospheric relative-humidity from the GOES 6.7 $\mu$m channel—Method and climatology for July 1987. *J. Geophys. Res.,* **98,** 16 669–16 688.

——, and I. M. Held, 2006: An assessment of climate feedbacks in coupled ocean–atmosphere models. *J. Climate,* **19,** 3354–3360.

——, R. T. Wetherald, G. L. Stenchikov, and A. Robock, 2002: Global cooling after the eruption of Mount Pinatubo: A test of climate feedback by water vapor. *Science,* **296,** 727–730.

——, D. D. Turner, B. M. Lesht, and L. M. Miloshevich, 2004: An analysis of satellite, radiosonde, and lidar observations of upper tropospheric water vapor from the Atmospheric Radiation Measurement Program. *J. Geophys. Res.,* **109,** D04105, doi:10.1029/2003JD003828.

——, D. L. Jackson, V. Ramaswamy, M. D. Schwarzkopf, and X. L. Huang, 2005: The radiative signature of upper tropospheric moistening. *Science,* **310,** 841–844.

Spencer, R., and W. D. Braswell, 1997: How dry is the tropical free troposphere? Implications for global warming theory. *Bull. Amer. Meteor. Soc.,* **78,** 1097–1106.

Spichtinger, P., K. Gierens, and W. Read, 2002: The statistical distribution law of relative humidity in the global tropopause region. *Meteor. Z.,* **11,** 83–88.

Steiner, A. K., and G. Kirchengast, 2005: Error analysis for GNSS radio occultation data based on ensembles of profiles from end-to-end simulations. *J. Geophys. Res.,* **110,** D15307, doi:10.1029/2004JD005251.

Tompkins, A. M., 2002: A prognostic parameterization for the subgrid-scale variability of water vapor and clouds in large-scale models and its use to diagnose cloud cover. *J. Atmos. Sci.,* **59,** 1917–1942.

Tuck, A. F., S. J. Hovde, K. K. Kelly, M. J. Mahoney, M. H. Proffitt, E. C. Richard, and T. L. Thompson, 2003: Exchange between the upper tropical troposphere and the lower stratosphere studied with aircraft observations. *J. Geophys. Res.,* **108,** 4734, doi:10.1029/2003JD003399.

Waters, J. W., and Coauthors, 2006: The earth observing system microwave limb sounder (EOS-MLS) on the Aura satellite. *IEEE Trans. Geosci. Remote Sens.,* **44,** 1075–1092.

Wu, X. B., J. Li, W. J. Zhang, and F. Wang, 2005: Atmospheric profile retrieval with AIRS data and validation at the ARM CART site. *Adv. Atmos. Sci.,* **22,** 647–654.

Zhang, C., B. E. Mapes, and B. Soden, 2003: Bimodality of tropical upper tropospheric humidity. *Quart. J. Roy. Meteor. Soc.,* **129,** 2847–2866.